

Hardness Enhancement in Al-Si Alloy Through Combined Pressing and Heat Treatment with Coconut Shell Charcoal Media

Masyrukan¹, Agung Setyo Darmawan¹, Agus Yulianto¹, Abdul Hamid²

¹*Mechanical Engineering Department, Universitas Muhammadiyah Surakarta, Surakarta, Indonesia.*

²*Technology Education Department, Universiti Tun Hussein Onn Malaysia, Johor Darul Ta'zim, Malaysia*

Email: masyrukan@ums.ac.id

Abstract: The study investigated the enhancement of hardness in Al-Si alloy through a combination of pressing and heat treatment using coconut shell charcoal media. Utilizing a novel approach, the alloy specimens were subjected to heat treatment at 450°C followed by a brief pressing process and an artificial aging treatment. The results revealed a significant increase in surface hardness from 76.32 VHN to 133 VHN, attributed to the formation of aluminum carbide (Al_4C_3) and aluminum oxide (Al_2O_3) on the alloy surface. This suggested that the combined treatment process effectively improves the mechanical properties of the Al-Si alloy, making it suitable for applications requiring enhanced wear resistance and durability.

Keywords: Al-Si, carburizing, coconut shell, hardness.

1. Introduction

The enhancement of material properties through various treatment processes is a critical aspect of materials engineering. Aluminum-silicon (Al-Si) alloys, known for their excellent castability, corrosion resistance, and mechanical properties, are widely used in automotive, aerospace, and other engineering applications [1–3]. To further improve these properties, particularly hardness, researchers have explored numerous heat treatment techniques [4]. Among these, combining heat treatment with pressing and using alternative media such as coconut shell charcoal has garnered significant attention. This study focuses on the impact of pressing addition to the heat treatment process at a temperature of 400°C using coconut shell charcoal media on the hardness of Al-Si alloy.

Heat treatment is a well-established method to enhance the mechanical properties of alloys. It involves heating and cooling cycles that alter the microstructure of the material, thereby improving its hardness, strength, and ductility [5–8]. In the case of Al-Si alloys, heat treatment processes such as solution heat treatment, quenching, and aging are commonly employed [9–11]. However, the integration of pressing into the heat treatment process is a relatively novel approach that aims to further refine the microstructure and enhance the mechanical properties.

The use of coconut shell charcoal as a treatment medium is particularly interesting due to its unique properties. Coconut shell charcoal is known for its high carbon content and porosity, which can influence the thermal and chemical interactions during the heat treatment process [12–15]. When used in conjunction with pressing, it is hypothesized that the coconut shell charcoal can facilitate better diffusion of alloying elements and impurities, leading to a

more uniform and refined microstructure. This study aims to investigate these effects in detail, focusing on the resultant hardness of the Al-Si alloy.

Pressing during the heat treatment process applies mechanical stress to the material, potentially enhancing the densification and reducing porosity [16–19]. This mechanical action, combined with the thermal effects of heat treatment, can significantly alter the microstructure, potentially leading to improved hardness [20]. The exact mechanisms through which pressing and coconut shell charcoal media influence the hardness of Al-Si alloys remain an area of active research [21–23]. This study seeks to elucidate these mechanisms through a series of controlled experiments and detailed microstructural analyses.

Understanding the combined effects of pressing and heat treatment with coconut shell charcoal media on Al-Si alloys is not only academically intriguing but also holds significant practical implications. Enhanced hardness can lead to better wear resistance and longer service life of components made from these alloys, making them more suitable for demanding applications [24–27]. Additionally, utilizing coconut shell charcoal, a renewable and environmentally friendly material, aligns with the growing emphasis on sustainable manufacturing practices [28–30].

Hardness is one of the important properties of materials used as components of structures that are under compressive stress [31–35]. This research is structured to provide a comprehensive analysis of how pressing and coconut shell charcoal media influence the hardness of Al-Si alloys treated at 400°C. By combining experimental data with theoretical insights, the study aims to offer a deeper understanding of the material behaviors and potential improvements in alloy performance. The findings are expected to contribute to the development of more efficient and sustainable heat treatment processes for Al-Si alloys and potentially other similar materials.

2. Materials and Methods

2.1 Materials

The primary material used in this study is an Al-Si alloy, chosen for its common use in the automotive and aerospace industries due to its excellent mechanical properties and castability. The specific composition of the alloy was verified using spectroscopic analysis (Table 1). Coconut shell charcoal was selected as the medium for heat treatment, sourced from a local supplier. The charcoal was ground into a fine powder to increase its surface area, ensuring a uniform and consistent interaction with the Al-Si alloy during the heat treatment process.

Al	Si	Cu	Ni	Mg	Fe	Mn	Zn	Ti	Cr	V	Zr
2.20	3.08	.296	.276	.156	.663	.113	.111	.041	.026	.012	.082

Source: Authors

2.2 Sample Preparation

The Al-Si alloy was machined into standardized test specimens, each measuring 10 mm x 10 mm x 50 mm, to facilitate uniform testing conditions. The specimens were polished using a series of abrasive papers and finished with a polishing cloth to achieve a mirror-like surface, removing any surface oxides or contaminants. This preparation ensured that the effects of the heat treatment could be accurately assessed without interference from surface impurities. The

specimens were then divided into two groups: the untreated Al-Alloy and the material that underwent the combined pressing and heat treatment process with coconut shell charcoal media.

2.3 Heat Treatment Process

The heat treatment was performed in a muffle furnace capable of maintaining precise temperature control. For the experimental group, the specimens were embedded in coconut shell charcoal powder within the furnace. The specimens were heated to 450°C at a controlled heating rate of 10°C per minute. This initial heating phase is crucial as it allows the material to reach the necessary temperature for the subsequent processes. After the 75-minute heating period, the specimen is carefully removed from the oven. The next step involves a pressing process, which is brief but significant, lasting only 45 seconds. During this time, a pressing load of 20 kg is applied to the specimen to alter the microstructure or relieve internal stresses in the material. Following the pressing process, the specimen undergoes an artificial aging process at 200°C for 20 minutes. This aging process involves the precipitation of certain phases to enhance mechanical properties. After the aging period, the specimen is cooled gradually inside the oven to avoid thermal shocks or undesirable residual stresses that could compromise the material's integrity. This sequence of heating, pressing, aging, and controlled cooling is meticulously designed to achieve the desired physical and mechanical properties in the specimen. The heat treatment process is illustrated in Figure 1.

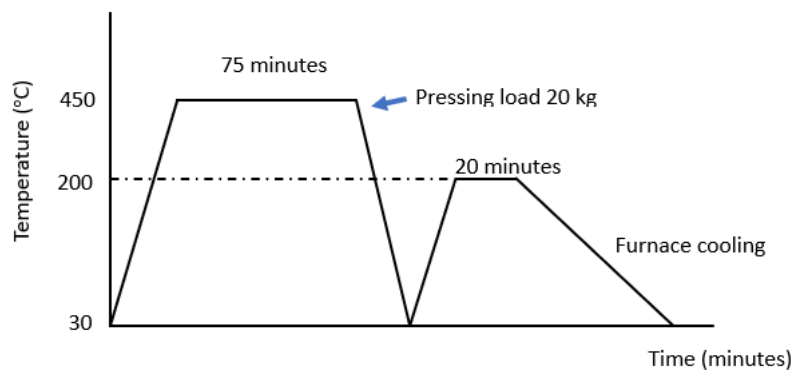


Figure 1. Schematic of the heat treatment and pressing process using Coconut Shell Charcoal media.

2.4 Density Testing

The density test was carried out on the untreated Al-Alloy and the material that underwent the combined pressing and heat treatment process with coconut shell charcoal media. The process involved preparing the test sample, accurately measuring its mass with a digital scale, and determining its volume using a measuring cup. The density was then calculated by dividing the mass by the volume. This straightforward yet precise method ensures reliable density values, aiding in material characterization and quality assurance for industrial and research applications.

2.5 Hardness Testing

The hardness of each specimen was measured using a Vickers hardness tester. Indentations were made at multiple locations on each specimen to obtain a comprehensive hardness profile, with an applied load of 10 kg and a dwell time of 15 seconds for each indentation. The average hardness values were calculated to ensure statistical reliability.

Additionally, microhardness testing was conducted on cross-sectional samples using a micro-Vickers hardness tester to evaluate the hardness variation within the material. This provided insights into the depth of hardness penetration and the uniformity of the treatment effects.

2.6 Microstructural Analysis

To correlate the hardness results with the microstructural changes, a detailed microstructural analysis was performed. Specimens from both the untreated and heat-treated Al-Si alloy were sectioned, mounted, and polished for microscopic examination. Optical microscopy was used to observe the general microstructure of untreated Al-Si alloy. Scanning electron microscopy (SEM) was used to analyze the surface layer, the boundary between the surface layer and substrate, and the substrate after the heat treatment and pressing process using Coconut Shell Charcoal media. Energy-dispersive X-ray spectroscopy (EDS) was used in conjunction with SEM to identify elemental compositions and detect any carbon infiltration from the coconut shell charcoal. The microstructural data were compared with the hardness measurements to conclude the effectiveness of the combined pressing and heat treatment process in enhancing the hardness of the Al-Si alloy.

3. Results and Discussions

3.1 Microstructural Analysis

The microstructure of the Al-Si alloy reveals the presence of the α -Al and β -Si phases (Figure 2). In the micrograph, the alpha phase appeared as a continuous matrix composed of aluminum. The β -Si phase was dispersed within this matrix, manifesting as dark needle-like particles. These silicon particles were embedded within the aluminum matrix, providing the alloy with improved wear resistance and strength. The distribution and morphology of these phases significantly influence the mechanical properties and overall performance of the alloy [36,37].

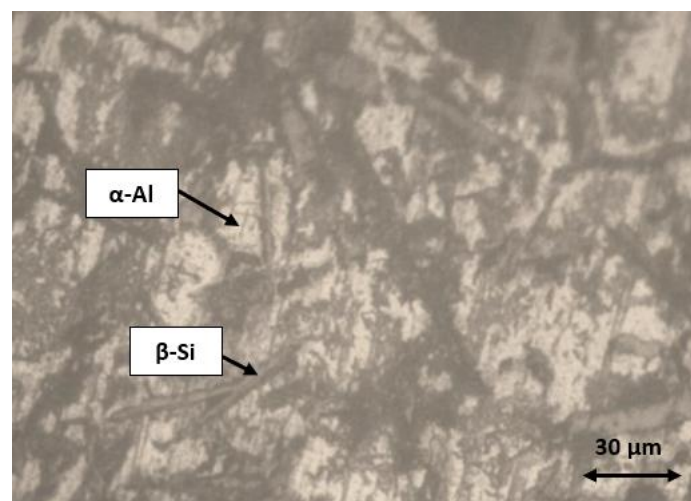
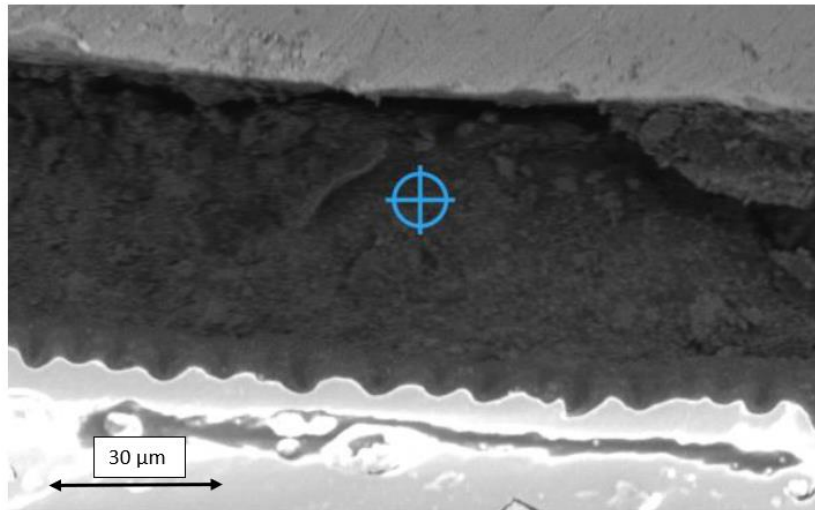


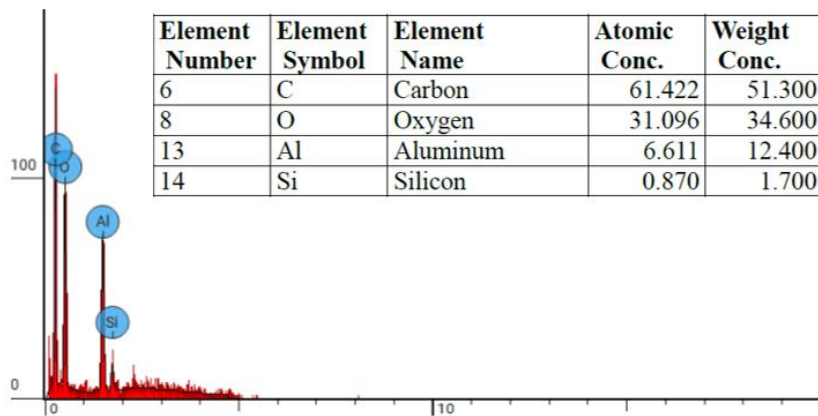
Figure 2. *The microstructure of the Al-Si alloy.*

After the heat treatment process with Coconut Shell Charcoal media combined with pressing. Metallographic observations were carried out using SEM-EDS. Metallography test results using SEM-EDS at the surface layer are shown in Figure 3. Figure 3a shows the location of the spectrum at the surface layer. EDS analysis of a carburized Al-Si alloy (Figure 3b) provides insight into the elemental composition and possible compounds present in the alloy's surface layer. The reported EDS results indicated significant concentrations of carbon (51.3%),

oxygen (34.6%), aluminum (12.4%), and silicon (1.7%). These results suggested the formation of specific compounds and the microstructural changes due to the carburizing process.



(a)



(b)

Figure 3. Metallography test results using SEM-EDS at surface layer (a) spectrum, (b) EDS Line analysis

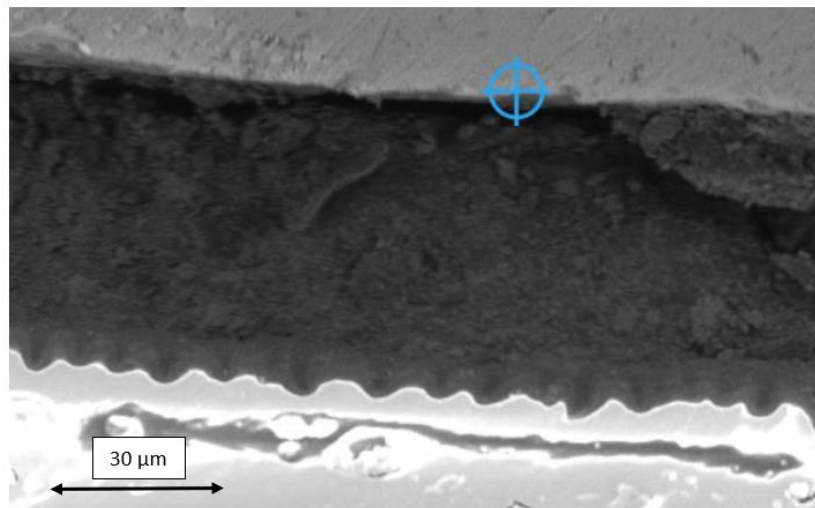
The high carbon content (51.3%) strongly indicates the formation of aluminum carbide (Al_4C_3) as a primary compound [38]. Aluminum carbide was formed when carbon diffused into the aluminum matrix during carburizing and this compound was characterized by its high hardness and brittleness. The presence of aluminum (12.4%) supported this formation, as aluminum carbide required a substantial amount of aluminum from the base alloy to combine with the introduced carbon.

The presence of oxygen (34.6%) was significant and suggested the formation of aluminum oxide (Al_2O_3) [39]. Aluminum oxide forms a protective layer on the surface, which can enhance the corrosion resistance of the alloy but may interfere with the diffusion of carbon during carburizing, leading to a complex microstructure with both carbides and oxides present.

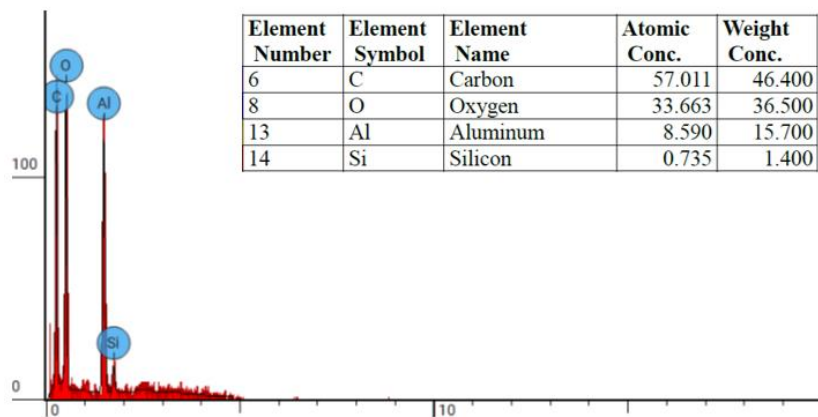
The silicon content (1.7%) was relatively low compared to the other elements. However, this small amount of silicon can still form silicon carbide (SiC) if conditions allow for silicon to react with carbon [40,41]. Silicon carbide is another hard compound, though its formation is less likely given the much lower concentration of silicon compared to aluminum and carbon. Additionally, silicon may also be present as part of the original Al-Si alloy matrix, where it

enhances the mechanical properties of aluminum without reacting to form significant amounts of new compounds during carburizing.

Figure 4 shows metallography test results using SEM-EDS at the boundary between the surface layer and the substrate. The location of the spectrum is shown in Figure 4a. Analyzing the EDS result at the boundary between the compound layer and the substrate of a carburized Al-Si alloy reveals critical insights into the elemental distribution and the potential compounds formed at this interface (Figure 4b). The EDS results show the presence of carbon (46.4%), oxygen (36.5%), aluminum (15.7%), and silicon (1.4%). These concentrations suggested specific microstructural changes and the formation of compounds that influence the properties of this transitional zone.



(a)



(b)

Figure 4. Metallography test results using SEM-EDS at the boundary between the surface layer and the substrate (a) spectrum, (b) EDS Line analysis

The substantial carbon content (46.4%) at the boundary indicated that the diffusion of carbon into the substrate is still significant but slightly lower than in the outer compound layer. This suggests the presence of aluminum carbide (Al_4C_3) extending from the surface into the substrate. The formation of aluminum carbide at this boundary continues to enhance the surface hardness and wear resistance of the alloy, although the concentration gradient indicated a transition zone where the carbide phase became less pronounced as it moved deeper into the substrate [42].

The high oxygen content (36.5%) remains notable at this boundary, implying that aluminum oxide (Al_2O_3) was still present as a thin layer or dispersed particles within the aluminum matrix. This oxide layer can contribute to the corrosion resistance and overall stability of the carburized layer. The presence of aluminum oxide at the boundary indicates that the oxidation process affected both the outer compound layer and the transitional zone, creating a protective barrier that could influence the diffusion dynamics of carbon and other elements.

Aluminum (15.7%) is relatively more concentrated at this boundary compared to the outer compound layer, suggesting a gradual transition from the aluminum-rich substrate to the carbon-enriched surface. This aluminum presence is essential for the formation of aluminum carbide and aluminum oxide, maintaining the structural integrity of the alloy while accommodating the infused carbon and oxygen. The increased aluminum content at this boundary may indicate a region where the microstructure begins to transition back to the original aluminum matrix, with less carbide formation compared to the outer layer.

The silicon content (1.4%) remained low but consistent with the results from the outer compound layer. This suggested that silicon does not significantly migrate or react during the carburizing process remaining as part of the original Al-Si alloy microstructure. Silicon's presence, albeit low, could still contribute to the mechanical properties of the boundary layer, potentially forming minor amounts of silicon carbide (SiC) or remaining as silicon particles within the aluminum matrix.

Figure 5a shows the spectrum on the substrate. Analyzing the EDS results (Figure 5b) at the substrate of a carburized Al-Si alloy provided insight into the elemental composition and potential microstructural characteristics deeper within the alloy, beyond the immediate influence of the carburizing process. The EDS results for the substrate show carbon (24.7%), oxygen (8.2%), aluminum (67.1%), and no detectable silicon (0%). These concentrations reflected the diffusion dynamics and interactions of elements as they moved further from the carburized surface layer into the bulk alloy.

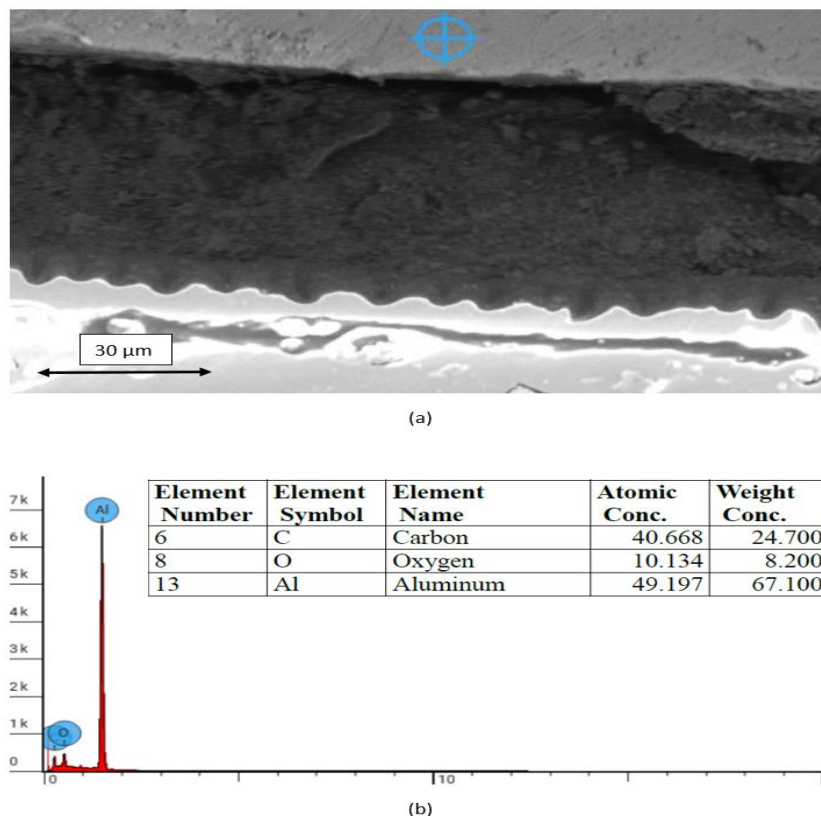


Figure 5. Metallography test results using SEM-EDS at the substrate (a) spectrum, (b) EDS Line analysis.

The presence of carbon at 24.7% within the substrate indicated that carbon diffusion extends significantly into the alloy, albeit at a reduced concentration compared to the surface and boundary layers. This lower carbon concentration suggested that while some aluminum carbide (Al_4C_3) might still form, its presence would be less pronounced compared to the surface layers. The reduced carbide content at this depth results in a more gradual transition back to the original aluminum matrix, ensuring that the substrate maintains more of its ductile properties.

The oxygen content at 8.2% suggested that some aluminum oxide (Al_2O_3) is present within the substrate, although its concentration was much lower compared to the surface and boundary layers. This implies that the oxidation effect diminished as they moved deeper into the substrate, resulting in a less pronounced oxide layer. The presence of aluminum oxide at this depth could still contribute to localized improvements in corrosion resistance and stability, but its impact on the overall microstructure would be minimal.

Aluminum, at 67.1%, was the dominant element in the substrate, reflecting the primary composition of the original Al-Si alloy. This high concentration indicated that the bulk of the alloy's microstructure was primarily aluminum, with carbon and oxygen present in smaller amounts. The aluminum-rich substrate ensured that the mechanical properties of the base alloy, such as ductility and toughness, were largely retained, providing a supportive structure for the harder carburized surface layers [43].

The absence of silicon (0%) in the EDS results was notable. This could be due to the limitations of the EDS technique in detecting low concentrations of silicon or a localized depletion of silicon in the analyzed area. In the original Al-Si alloy, silicon typically enhances strength and reduces density [44]. The lack of detectable silicon in the substrate analysis suggested that the carburizing process did not significantly alter the silicon distribution, and any existing silicon might remain integrated into the aluminum matrix or present in amounts below the detection threshold.

3.2 Density Testing

The density test results for the untreated and heat-treated Al-Si alloy revealed a minimal change in density after the carburizing treatment (Figure 6). Specifically, the untreated Al-Si alloy had a density of 2.598 grams/cm³, while the carburized alloy showed a slightly increased density of 2.599 grams/cm³. This minute change provides valuable insights into the effects of the carburizing process on the alloy's microstructure and composition.

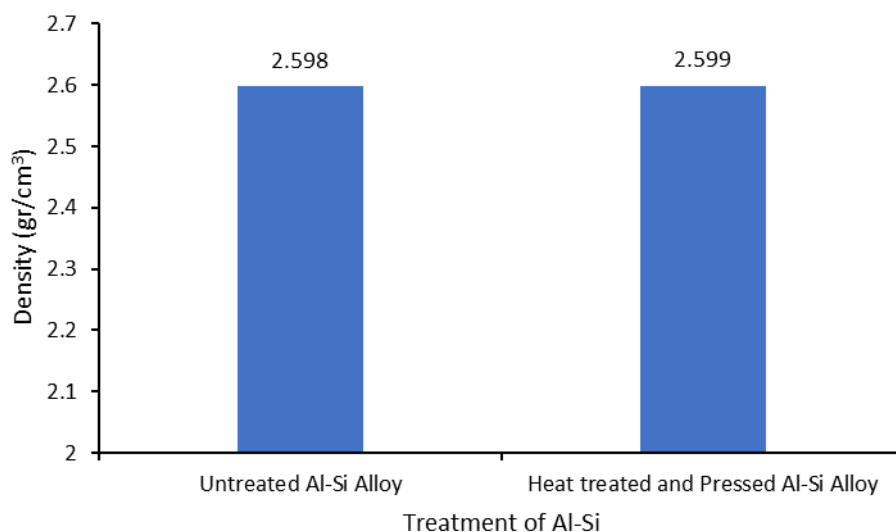


Figure 6. *The effect of the heat treatment process and pressing with Coconut Shell Charcoal media on density.*

The negligible increase in density (0.001 grams/cm³) suggested that the carburizing process primarily affected the surface layer of the Al-Si alloy without significantly altering the bulk properties. Carburizing involves infusing carbon into the surface of the alloy to form compounds such as aluminum carbide (Al₄C₃). These carbides were denser than the base aluminum alloy, leading to a slight increase in overall density [45]. However, the minimal change indicated that the carburized layer was thin relative to the bulk material, and the amount of carbon diffused into the alloy was relatively small compared to the total volume of the sample.

The slight increase in density can also be attributed to the formation of other compounds, such as aluminum oxide (Al₂O₃), which may form due to the presence of oxygen during the carburizing process. Aluminum oxide was also denser than the base aluminum alloy, contributing marginally to the overall density increase. The fact that this increase was so small suggested that these compounds were localized to the surface and did not penetrate deeply into the substrate.

3.3 Hardness Testing

The results of the Vickers hardness test for the untreated and carburized Al-Si alloy show a significant increase in hardness due to the carburizing treatment (Figure 7). The untreated Al-Si alloy had a hardness of 76.32 VHN, whereas the carburized alloy exhibited a hardness of 133 VHN. This substantial increase in hardness provided important insights into the effects of the carburizing process on the alloy's surface properties.

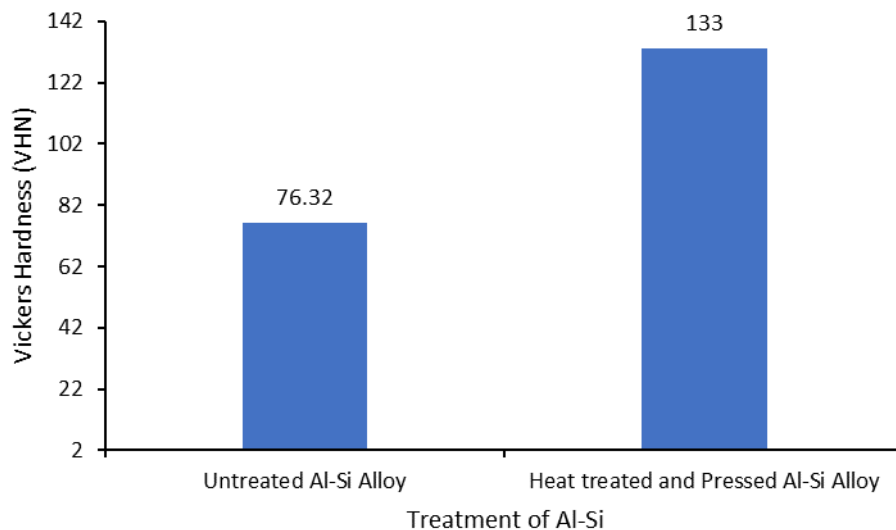


Figure 7. The effect of the heat treatment process and pressing with Coconut Shell Charcoal media on hardness.

The increase from 76.32 VHN to 133 VHN demonstrated the effectiveness of carburizing in enhancing the surface hardness of the Al-Si alloy. Carburizing involves the diffusion of carbon into the alloy's surface, leading to the formation of hard carbides, such as aluminum carbide (Al₄C₃). These carbides significantly enhanced the surface hardness due to their higher hardness compared to the base aluminum alloy [46]. The significant increase in hardness indicated that a sufficient amount of carbon had diffused into the surface, forming a durable carbide layer.

The minor increase in density observed in the density test, coupled with the significant increase in hardness, suggested that the carburizing treatment primarily affected the surface

layer without substantially altering the bulk properties of the alloy. The hardness improvement was concentrated in this thin carburized layer.

The considerable increase in hardness also implies improved performance in applications subjected to high friction, wear, and mechanical stresses. The carburized surface can better resist deformation, scratching, and wear, thereby extending the component's lifespan and maintaining its integrity under demanding conditions [47]. The enhanced hardness made the Al-Si alloy more suitable for use in automotive, aerospace, and industrial applications where durability and resistance to surface damage are critical.

4. Conclusion

The EDS results of the carburized Al-Si alloy suggested that aluminum carbide (Al_4C_3) was the primary compound formed due to the high carbon and aluminum content, while the significant presence of oxygen indicates the formation of aluminum oxide (Al_2O_3). At the boundary between the carburized layer and the substrate, EDS analysis revealed a complex interplay of these compounds, with carbon and oxygen playing crucial roles. In the substrate, there was a reduced but notable presence of carbon, moderate oxygen, and dominant aluminum, with no detectable silicon. The density test showed a minor increase, indicating the formation of a thin, dense surface layer that enhanced the alloy's surface characteristics, such as hardness and wear resistance, without significantly affecting the bulk properties. Vickers hardness test results further confirm that carburizing significantly increased the surface hardness from 76.32 VHN to 133 VHN, primarily due to the formation of hard carbide phases, achieving this improvement while maintaining the overall integrity of the alloy's core properties.

Acknowledgments

The authors would like to acknowledge the materials engineering research center and materials laboratory from the mechanical engineering department, Muhammadiyah University of Surakarta which has facilitated the research.

Disclosure Statement

The authors declare no conflict of interest related to this study. All aspects of the research, including the design, data collection, analysis, and publication, were conducted independently of any funding or external influence. The authors have no financial or personal relationships that could have inappropriately influenced or biased the work presented in this manuscript.

References

1. Karthikeyan N, Krishnan BR, VembathuRajesh A, Vijayan V. Experimental analysis of Al-Cu-Si metal matrix composite by powder-metallurgy process. *Mater Today Proc* 2021;37:2770–4. <https://doi.org/10.1016/j.matpr.2020.08.643>.
2. Rao BS, Rao TB. Mechanical and Tribological Properties of 3D printed Al-Si alloys and composites: a Review. *Silicon* 2022;14:5751–82. <https://doi.org/10.1007/s12633-021-01340-9>.
3. Sanath MN, Nihal CL, Prabhuling, Shivaprasad PM, Puneeth HV, Srinath MK. Review on Corrosion studies of Heat Treated Al-Si Alloy. *IOP Conf Ser Mater Sci Eng* 2022;1258:012028. <https://doi.org/10.1088/1757-899X/1258/1/012028>.
4. Muttahar MIZ, Virdhian S, Putra PA, Djuanda DR, Afrilinda E, Genesar A. Mechanical Properties Enhancement of Al-Si-Cu-Fe Alloy Through Aging Treatment Variations. *Metalurgi* 2020;35:105. <https://doi.org/10.14203/metalurgi.v35i3.571>.

5. Singh B, Anupama B, Kalra R, Dhamija K, Kareem A, Kumar M. Investigating the Effects of Advanced Heat Treatment Techniques on the Mechanical Properties of Cast Components. *E3S Web of Conferences* 2023;430:01112. <https://doi.org/10.1051/e3sconf/202343001112>.
6. Chandra Kandpal B, Gupta DK, Kumar A, Kumar Jaisal A, Kumar Ranjan A, Srivastava A, et al. Effect of heat treatment on properties and microstructure of steels. *Mater Today Proc* 2021;44:199–205. <https://doi.org/10.1016/j.matpr.2020.08.556>.
7. Bharti S, Arora G, Singh K, Varshney S. Effect of Heat Treatment Processes on Metals and Alloys-A Review. *International Journal Of Advanced Production And Industrial Engineering* 2020;5:54–63. <https://doi.org/10.35121/ijapie202004247>.
8. Hasibur Rahaman. Comparative Failure Analysis of Ferrous and Non-Ferrous Heat-Treated Materials. *International Journal For Multidisciplinary Research* 2023;5. <https://doi.org/10.36948/ijfmr.2023.v05i03.3849>.
9. Singh P, Singh RK, Das AK. Optimization of heat treatment cycle for cast-Al6082 alloy to enhance the mechanical properties. *Engineering Research Express* 2024;6:015036. <https://doi.org/10.1088/2631-8695/ad1cb1>.
10. Kuchariková L, Tillová E, Švecová I. Consequences of Inappropriate Temperatures of the Solution Heat Treatment in Al-Si-Cu Cast Alloys. *Defect and Diffusion Forum* 2020;405:357–64. <https://doi.org/10.4028/www.scientific.net/DDF.405.357>.
11. Schmid F, Dumitraschkewitz P, Kremmer T, Uggowitzner PJ, Tosone R, Pogatscher S. Enhanced aging kinetics in Al-Mg-Si alloys by up-quenching. *Commun Mater* 2021;2:58. <https://doi.org/10.1038/s43246-021-00164-9>.
12. Kabir Ahmad R, Sulaiman SA. Carbonization of Coconut Shell Biomass in a Downdraft Reactor: Effect of Temperature on the Charcoal Properties. *Sains Malays* 2021;50:3705–17. <https://doi.org/10.17576/jsm-2021-5012-20>.
13. Praswanto DH, Asroni M, Priyasmanu T, Prihatmi TN. Heat Flux Condensation on Coconut Shell Activated Charcoal Porous Media. *Journal Of Science And Applied Engineering* 2020;3. <https://doi.org/10.31328/jsae.v3i2.1770>.
14. Arief RK, Armila A, Liswardi A, Yahya H, Warimani MS, Putera P. Coconut Shell Carbonization Process Using Smokeless Kiln. *Journal of Applied Agricultural Science and Technology* 2023;7:82–90. <https://doi.org/10.55043/jaast.v7i2.135>.
15. Ahmad RK, Sulaiman SA, Yusuf SB, Dol SS, Umar HA, Inayat M. The Influence Of Pyrolysis Process Conditions On The Quality Of Coconut Shells Charcoal. *Platform : A Journal of Engineering* 2020;4:73. <https://doi.org/10.61762/pajevol4iss1art7663>.
16. Sözbir GD, Bektas I, Ak AK. Influence of combined heat treatment and densification on mechanical properties of poplar wood. *Maderas Ciencia y Tecnología* 2019;0–0. <https://doi.org/10.4067/S0718-221X2019005000405>.
17. Qin S, Herzog S, Kaletsch A, Broeckmann C. Effects of Pressure on Microstructure and Residual Stresses during Hot Isostatic Pressing Post Treatment of AISI M50 Produced by Laser Powder-Bed Fusion. *Metals (Basel)* 2021;11:596. <https://doi.org/10.3390/met11040596>.
18. Kluczyński J, Śnieżek L, Grzelak K, Oziębło A, Perkowski K, Torzewski J, et al. Hot isostatic pressing influence on the mechanical properties of selectively laser-melted 316L steel. *Bulletin of the Polish Academy of Sciences Technical Sciences* 2020;68:1413–24. <https://doi.org/10.24425/bpasts.2020.135396>.
19. Schukina LP, Bolyukh VF, Lihezin SL, Pitak YaM. Dynamic pressing as a way of intensification of structural-phase transformations during sintering of ceramic materials. *Scientific Research on Refractories and Technical Ceramics* 2021;121:162–8. <https://doi.org/10.35857/2663-3566.121.17>.

20. Gu T, Xu F, Zhao Y, Hou H, Liu J. Effects of high pressure heat treatment on microstructure and mechanical properties of aluminum bronze. *Mater Res Express* 2019;6:096508. <https://doi.org/10.1088/2053-1591/ab2a4d>.
21. Dash SS, Chen D. A Review on Processing–Microstructure–Property Relationships of Al-Si Alloys: Recent Advances in Deformation Behavior. *Metals (Basel)* 2023;13:609. <https://doi.org/10.3390/met13030609>.
22. Choudhary C, Sahoo KL, Roy H, Mandal D. Effect of Grain Refiner on Microstructural Feature Influence Hardness and Tensile Properties of Al-7Si Alloy. *J Mater Eng Perform* 2022;31:3262–73. <https://doi.org/10.1007/s11665-021-06413-9>.
23. Guo F, Wang R, Peng C, Cai Z, Liu Y, Feng Y, et al. Effects of Cu and Mg alloying on the microstructure and properties of Al–12Si alloy prepared by spray forming. *Journal of Materials Science: Materials in Electronics* 2020;31:5416–24. <https://doi.org/10.1007/s10854-020-03103-5>.
24. Jin B-R, Ha D-W, Jeong C-Y. Effect of Solution Treatment on the Hardness and Tensile Properties of Al–Mg–Si Alloys for Automotive Chassis. *Mater Trans* 2019;60:815–23. <https://doi.org/10.2320/matertrans.M2018368>.
25. Ammar HR, Samuel AM, Doty HW, Samuel FH. Effect of Iron, Copper and Heat Treatments on the Microstructure and Tensile Properties of Al-Si-Based Alloys. *International Journal of Metalcasting* 2022;16:1101–21. <https://doi.org/10.1007/s40962-021-00677-6>.
26. Darmawan AS, Purboputro PI, Sugito B, Febriantoko BW, Yulianto A, Suprpto, et al. Improving surface hardness and wear resistance of commercially pure titanium by plasma nitriding process, 2023, p. 040006. <https://doi.org/10.1063/5.0125860>.
27. Darmawan AS, Purboputro PI, Febriantoko BW. The effect of composition on hardness and wear resistance of rice plant fiber reinforced composite as a material of brake lining. *IOP Conf Ser Mater Sci Eng* 2020;771:012069. <https://doi.org/10.1088/1757-899X/771/1/012069>.
28. Rudiyanto B, Agustina IR, Ulma Z, Prasetyo DA, Hijriawan M, Piluharto B, et al. Utilization of Cassava Peel (*Manihot utilissima*) Waste as an Adhesive in the Manufacture of Coconut Shell (*Cocos nucifera*) Charcoal Briquettes. *International Journal of Renewable Energy Development* 2023;12:270–6. <https://doi.org/10.14710/ijred.2023.48432>.
29. Ajien A, Idris J, Md Sofwan N, Husen R, Seli H. Coconut shell and husk biochar: A review of production and activation technology, economic, financial aspect and application. *Waste Management & Research: The Journal for a Sustainable Circular Economy* 2023;41:37–51. <https://doi.org/10.1177/0734242X221127167>.
30. Guerra MA, Iturralde F. Literature Review Of Coconut Shell And Fibers In Pavement Design. *Proceedings of International Structural Engineering and Construction* 2024;11. [https://doi.org/10.14455/ISEC.2024.11\(1\).MAT-07](https://doi.org/10.14455/ISEC.2024.11(1).MAT-07).
31. Hariningsih, Gustiani D, Sutiyoko. Effect Of Quenching Media Variations On The Hardness And Microstructures Of Aisi O1 Tool Steel. *Media Mesin: Majalah Teknik Mesin* 2023;24:82–9. <https://doi.org/10.23917/mesin.v24i2.22191>.
32. Sugito B, Hariyanto A, Anggono AD, Subroto, Darmawan AS. Influence of tool speed on the friction stir welding joint of aluminium and steel with single weld line. *IOP Conf Ser Mater Sci Eng* 2019;674:012064. <https://doi.org/10.1088/1757-899X/674/1/012064>.
33. Anggono AD, Kholis N, Ngafwan. Structure and Mechanical Properties of Double Side Friction Stir Welded Aluminium AA6061 with the Addition of Cu Powder. *Materials Science Forum* 2022;1051:111–8. <https://doi.org/10.4028/www.scientific.net/MSF.1051.111>.

34. Hariningsih H, Lutiyaatmi L, Daryanto T. Effects of heat treatment on microstructure and hardness of D2 tools. *Applied Research and Smart Technology (ARSTech)* 2022;3:29–37. <https://doi.org/10.23917/arstech.v3i1.761>.
35. Purboputro PI, Darmawan AS. The Effect of Copper Particles Size on Hardness, Wear Resistance and Friction Coefficient of Fiberglass-Carbon Particles-Copper Particles Reinforced Composite. *Materials Science Forum* 2021;1029:49–55. <https://doi.org/10.4028/www.scientific.net/MSF.1029.49>.
36. Suheni, Syamsuri, Suryanto MB, Lillahulhaq Z. The effect of additional silicone and handling temperature on draw strength and microstructure in aluminum casting. *J Phys Conf Ser* 2021;1833:012047. <https://doi.org/10.1088/1742-6596/1833/1/012047>.
37. Callegari B, Lima TN, Coelho RS. The Influence of Alloying Elements on the Microstructure and Properties of Al-Si-Based Casting Alloys: A Review. *Metals (Basel)* 2023;13:1174. <https://doi.org/10.3390/met13071174>.
38. Gallyamova RF, Safiullin RL, Dokichev VA, Musin FF. Investigation Of Carbon-Aluminum Composite With A Barrier Coating On Carbon Fibers. *Petroleum Engineering* 2023;21:182–91. <https://doi.org/10.17122/ngdelo-2023-5-182-191>.
39. Wang J, Ling Y, Lu Z, Zhou Q, Wang R, Zhang Z. Enhanced formation of α -Al₂O₃ at low temperature on Cr/Al coating by controlling oxygen partial pressure. *Appl Surf Sci* 2020;515:146053. <https://doi.org/10.1016/j.apsusc.2020.146053>.
40. Aarnæs TS, Ringdalen E, Tangstad M. Silicon carbide formation from methane and silicon monoxide. *Sci Rep* 2020;10:21831. <https://doi.org/10.1038/s41598-020-79006-6>.
41. Abolpour B, Shamsoddini R. Mechanism of reaction of silica and carbon for producing silicon carbide. *Progress in Reaction Kinetics and Mechanism* 2020;45:146867831989141. <https://doi.org/10.1177/1468678319891416>.
42. Lee D, Kim J, Lee S-K, Kim Y, Lee S-B, Cho S. Effect of Boron Carbide Addition on Wear Resistance of Aluminum Matrix Composites Fabricated by Stir Casting and Hot Rolling Processes. *Metals (Basel)* 2021;11:989. <https://doi.org/10.3390/met11060989>.
43. Anand P, Rajesh D, Lenin N, Balaji V, Bupesh Raja VK, Palanikumar K. Enhancement of mechanical characterization of aluminum alloy with tungsten carbide metal matrix composite by particulate reinforcements. *Mater Today Proc* 2021;46:3690–2. <https://doi.org/10.1016/j.matpr.2021.01.848>.
44. Otani Y, Sasaki S. Effects of the addition of silicon to 7075 aluminum alloy on microstructure, mechanical properties, and selective laser melting processability. *Materials Science and Engineering: A* 2020;777:139079. <https://doi.org/10.1016/j.msea.2020.139079>.
45. Dwivedi SP. Microstructure and mechanical behaviour of Al/B₄C metal matrix composite. *Mater Today Proc* 2020;25:751–4. <https://doi.org/10.1016/j.matpr.2019.08.244>.
46. Vozniakovskii A, Kidalov S, Kol'tsova T. Development of composite material aluminum-carbon nanotubes with high hardness and controlled thermal conductivity. *J Compos Mater* 2019;53:2959–65. <https://doi.org/10.1177/0021998319829894>.
47. Bhadauria N, Pandey S, Pandey PM. Wear and enhancement of wear resistance – A review. *Mater Today Proc* 2020;26:2986–91. <https://doi.org/10.1016/j.matpr.2020.02.616>.